Aeroacoustics Conferences
30 May - 1 June, 2016, Lyon, France
22nd AIAA/CEAS Aeroacoustics Conference

Input-output analysis of heated axisymmetric turbulent jets

Jinah Jeun*, Joseph W. Nichols†, and Mihailo R. Jovanović‡
University of Minnesota, Minneapolis, MN 55455, USA

Motivated by the recent success of input-output analysis for predicting the aeroacoustics of axisymmetric isothermal high-speed turbulent jets, we apply input-output analysis to axisymmetric heated high-speed turbulent jets. We consider small perturbations about Reynolds-averaged Navier-Stokes (RANS) solutions of perfectly expanded turbulent jets with a range of jet Mach numbers and different levels of applied heating. We show that input-output analysis recovers the far-field acoustics of heated jets and may be used to identify the effects of heating on the sound generation mechanisms associated with turbulent jets. We also demonstrate that applied heating causes Mach wave radiation to occur even when the jet Mach number remains subsonic. By projecting high-fidelity large eddy simulation (LES) data onto an orthonormal set of input modes obtained about a time-averaged base flow, we find that sub-optimal modes are active for a $M_j = 1.5$ supersonic jet with $T_j/T_\infty = 1.74$.

Nomenclature

γ	Specific heat ratio
μ	Dynamic viscosity
ρ	Density
σ	Gain in amplitude
c	Speed of sound
D	Nozzle diameter
H	Transfer function
H^+	Adjoint of transfer function
M_a	Acoustic Mach number
M_j	Jet Mach number
n	Mode number
p	Pressure
R	Nozzle radius
Re	Reynolds number
s	Entropy
St	Jet Strouhal number, fD/u_j
St_a	Acoustic Strouhal number, fD/c_∞
t	Nozzle wall thickness
u	Velocity

Subscripts

∞	Ambient properties
j	Properties at the nozzle exit

I. Introduction

Noise produced by high-speed turbulent jets of airplane engines is a hazard to people working in close proximity. It is also a significant nuisance to nearby communities. This has resulted in strict noise regulations, motivating the need for quieter jet engines. Despite more than 60 years of research, however, jet noise prediction still remains challenging. This is partly because of the fact that even though exhaust jets are terrifyingly loud, the energy associated with acoustic radiation is small compared to the aerodynamic energy contained in jet turbulence.

While turbulence is a highly nonlinear, multi-scale, chaotic phenomenon, the noise produced by jet turbulence appears to be somewhat organized. In the early 1960s, Mollo-Christensen[1] first observed such order in the radiated acoustic field of subsonic jets and suggested a link between coherent structures inside

*Graduate Research Assistant, Department of Aerospace Engineering and Mechanics, University of Minnesota.
†Assistant Professor, Department of Aerospace Engineering and Mechanics, University of Minnesota.
‡Associate Professor, Department of Electrical and Computer Engineering, University of Minnesota.

the turbulence and instability waves in the base flow. These coherent structures, namely wavepackets, are well captured using parabolized stability equations (PSE),[2–6] global mode analysis,[7] as well as resolvent analysis.[8,9]

The state-of-the-art reduced order models for jet noise rely upon PSE analysis.[2–6] PSE-based models have met success at predicting the behavior of both the near-field and the far-field acoustics of supersonic jets but do not fully capture the far-field acoustics in the case of subsonic jets. This may be attributed to the underlying assumption of PSE analysis that perturbations initiate upstream and then grow via instability downstream. Such downstream marching, however, misses other types of linear dynamics.

In recent studies of axisymmetric isothermal turbulent jets,[10,11] it was shown that the optimal mode produced by input-output analysis reproduced wavepackets similar to those obtained by PSE analysis for supersonic jets, and this was responsible for nearly the entire acoustic response. For subsonic jets, input-output analysis also successfully predicted the far-field sound by including the contribution of sub-optimal modes. Furthermore, input-output analysis recovered significant sideline noise (perpendicular to the flow direction), which was almost entirely missing in PSE analysis. This further suggests that sideline noise may be understood in the context of the dynamics of coherent fluctuations.[6,12]

The present paper extends previous studies of input-output analysis[10,11,13] to study the aeroacoustics of axisymmetric heated turbulent jets. Increases in applied heating preserve coherent structures contained in jet turbulence[5] but may change the far-field noise generation pattern. We consider base flows over a range of jet and acoustic Mach numbers to identify the effect of applied heating on the sound generation mechanisms in terms of the optimal and sub-optimal modes that input-output analysis generates. In addition, by projecting a high-fidelity simulation database onto input modes, we quantify the role of sub-optimal modes under realistic forcing. We see that input-output modes reproduce the essential physics of heated jets, and thus could serve as a basis for reduced-order models of heated jet aeroacoustics.

II. Methodology

A. Base flows

To study effects of applied heating on infinitesimal perturbations in high-speed turbulent jets, we produce RANS solutions of axisymmetric, compressible, turbulent jets as base flows. We compute the RANS solutions using a modified $k-\varepsilon$ turbulence model with coefficients suggested by Thies and Tam[14] for high-speed jets. While the base flows are solutions to the RANS equations, we treat small perturbations about these base flows as governed by the linearized Euler equations, as will be discussed below. Even though the RANS solutions are not equilibrium solutions to the Euler equations, the wave-like perturbations that we obtain below and that are connected to acoustic radiation, are correlated over length scales much larger than the integral length scales of the turbulence. These modes then do not contribute significantly to the modification of the turbulent mean profile which is instead supported by Reynolds stresses involving much shorter length scales. Because of this scale separation, previous studies have found that linear analysis about turbulent mean base flows is able to predict experimental observations of coherent structures in jets rather closely.[6,15]

Figure 1 shows contours of axial velocity from a RANS calculation of supersonic heated jet with the jet Mach number $M_j = u_j/c_j = 1.5$ and the jet-to-ambient temperature ratio $T_j/T_\infty = 1.44$. The computational domain includes a free-slip cylindrical nozzle with radius $R = 1$ and wall thickness $t = 0.3R$, as shown by the white line extending from $x/R = -20$ to $x/R = 0$. The computational domain to compute RANS solutions extended from $x/R = -20$ to $x/R = 70$ in the axial direction and from $r/R = 0$ to $r/R = 50$ in the radial direction.

In addition to the RANS solution for the $M_j = 1.5$ jet, we also produce RANS solutions over a range of jet Mach numbers with different amounts of applied heating. As the core of the jet heats above ambient, the speed of sound c_j inside the jet increases, which means that the jet Mach number decreases for constant jet velocity u_j. In this case, it is useful to define another Mach number based on the constant speed of sound c_∞ in the ambient fluid. This is the acoustic Mach number, $M_a = u_j/c_\infty$. In our study we vary both the jet and acoustic Mach numbers such that $0.6 < M_j < 1.5$ and $0.6 < M_a < 2.0$. In each case, we consider only heated jets such that $M_j < M_a$. Also, in this study, we consider only ideally expanded jets such that $p_j/p_\infty = 1$ and assume the Reynolds number $Re = \rho_j u_j R/\mu = 10^6$ to be constant throughout the domain.

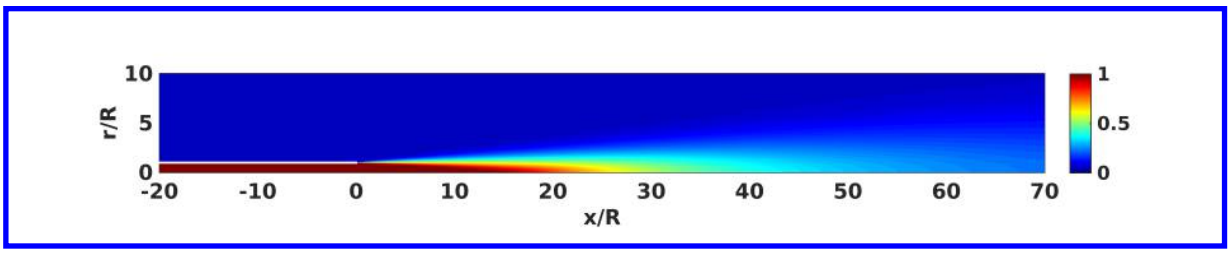

Figure 1. Contours of axial velocity from a RANS solution of a round $M_j = 1.5$ supersonic heated jet with $T_j/T_\infty = 1.44$. The velocity contours are normalized by the velocity at the nozzle exit at $x/R = 0$.

B. Linearized Euler Equations

We treat the dynamics of the system state $\mathbf{q} = \left[p; \mathbf{u}^T\right]^T$ where p and $\mathbf{u}$ denote the fluid pressure and velocity, respectively, as governed by the Euler equations. By introducing dimensionless variables defined with respect to the nozzle radius R, the jet velocity u_j, density ρ_j, and temperature T_j at the nozzle exit, the governing equations are written in dimensionless form as:

$$\frac{\partial p}{\partial t} + \mathbf{u} \cdot \nabla p + \rho c^2 \nabla \cdot \mathbf{u} = 0, \tag{1}$$

$$\frac{\partial \boldsymbol{u}}{\partial t} + \frac{1}{\rho} \nabla p + \boldsymbol{u} \cdot \nabla \boldsymbol{u} = 0. \tag{2}$$

Furthermore, the equation of state for an ideal gas becomes $\gamma {M_j}^2 p = \rho T$ where the jet Mach number is defined as $M_j = u_j/c_j$. Here, we assume that the ratio of specific heats $\gamma = 1.4$ is constant throughout the domain.

The dynamics of small fluctuations about base flows are examined using the linearized Euler equations (LEE). By decomposing the system state $\boldsymbol{q}$ into mean $\bar{()}$ and fluctuating parts $()'$ and neglecting higher-order terms, equations (1) and (2) are linearized as:

$$\frac{\partial p'}{\partial t} + \bar{\boldsymbol{u}} \cdot \nabla p' + \bar{\rho} \bar{c}^2 \nabla \cdot \boldsymbol{u}' + \gamma (\nabla \cdot \bar{\boldsymbol{u}}) p' = 0, \tag{3}$$

$$\frac{\partial \boldsymbol{u'}}{\partial t} + \frac{1}{\bar{\rho}} \nabla p' + \bar{\boldsymbol{u}} \cdot \nabla \boldsymbol{u'} + \boldsymbol{u'} \cdot \nabla \bar{\boldsymbol{u}} \; = \; 0, \tag{4}$$

We further express the LEE in matrix form as:

$$\frac{\partial q}{\partial t} = Aq, \tag{5}$$

where A is the linear operator, which depends on the base flow. For simplicity, we have dropped the primes and bold font.

C. Input-output analysis

In this section, we briefly introduce input-output analysis for the aeroacoustics of high-speed turbulent jets. For more details, we refer readers Ref. 11.

To analyze the linearized system (5), we impose the following wavepacket ansatz for perturbations:

$$q(x, r, \theta, t) = \hat{q}(x, r) e^{i(m\theta - \omega t)}, \tag{6}$$

where m is an azimuthal wavenumber and ω is the temporal frequency. In this paper, we consider axisymmetric ($m = 0$) disturbances only.

The high-speed jets we consider here are globally stable but convectively unstable in the form of wavepackets.[6] These jets are treated as amplifiers; they take external fluctuations as inputs and give back far-field

acoustics as outputs. To understand how input forcings map to outputs, we add an external forcing term f to the right hand side of the original equations (5) as:

$$\dot{q} = Aq + Bf, \tag{7}$$

$$y = Cq, \tag{8}$$

with y being output quantities of interest. Here, input-output analysis allows various combinations of matrices B and C, depending on input and output variables to be specified.

For inputs and outpus defined by $f = \hat{f}e^{zt}$ and $y = \hat{y}e^{zt}$, respectively, at a given temporal frequency ω, a transfer function H is written as:

$$H = C(zI - A)^{-1}B, \tag{9}$$

where $z = -i\omega$. Using singular value decomposition, H may be further decomposed as:

$$H = U\Sigma V^*, \tag{10}$$

where U and V are unitary matrices, and the superscript $(\ )^*$ denotes the complex-conjugate transpose. Here, Σ is a matrix whose diagonals are singular values, which are the gain in amplitude from input to output.

The singular values and the right-singular vectors of H may be efficiently computed by considering its adjoint operator H^+. Through the eigendecomposition of H^+H:

$$H^+H = B^*(z^*I - A^*)^{-1}C^*C(zI - A)^{-1}B, \tag{11}$$

the resulting eigenvalues represent the squares of the corresponding singular values σ of H. Note that for the transfer function H of the system, its adjoint operator H^+ maps outputs back onto inputs.

To evaluate the adjoint operator of the transfer function H^+, we adopt the continuous adjoint approach. Since it derives equations adjoint to the exact LEE first and then discretizes them later, the continuous approach supports the implementation of one-sided differences consistent with continuous derivatives near to the nozzle wall. In this way, we avoid numerical errors adjacent to the nozzle wall, which are observed in the discrete adjoint approach, to where far-field noise is highly sensitive.[16–19]

D. Numerical methods

The present study follows the similar approaches used in the authors' past papers.[10,11] The LEE are discretized using a fourth-order centered finite difference method. The grid is uniform in the axial direction and stretched in radial direction, clustered around the nozzle wall. Because of its non-dissipative nature, the centered finite difference method produces unphysical waves at the highest wavenumbers. To damp such spurious modes, we add weak fourth-order numerical filters. To describe the Sommerfeld radiation condition, we further employ numerical sponge layers at the boundaries of the numerical domain except for the centerline.[20,21]

In the previous section, we have shown that input-output analysis finds the gain in amplitude from inputs to outputs through the eigenvalue decomposition of H^+H. The largest eigenvalues of H^+H are computed using the free software package ARPACK, which is based upon the implicitly restarted Arnoldi method (IRAM),[22] and stored in descending order of magnitude. The matrix inversion of the resolvent operator $zI - A$ is evaluated by the sparse direct solver PARDISO, which is found from the Intel math kernel library. During the computation, the iterative Arnoldi method evaluates the resolvent multiple times for a fixed frequency. The factorization of the resolvent operator, however, is performed only once and may be reused in later time. Moreover, since the eigenvectors of H^+H are orthonormal to each other, the Arnoldi method converges rapidly.

In the study of input-output analysis for isothermal jets,[11] authors tested the independence of input-output analysis on the discretizations and numerical domain sizes. Based on that, we choose to use 576 and 288 grid points in the axial and radial directions, respectively, throughout the present study. Furthermore, the goal of the present study is to understand how forcing the velocity fluctuation equations (4) near to jet turbulence leads to far-field acoustic radiations. In this sense, we choose the matrix B to force the velocity equations in the neighborhood of the jet turbulence ($r/R < 2.90$) and the matrix C to select far-field pressure fluctuations ($r/R > 8.70$).

III. Results

A. Optimal and sub-optimal modes of heated jets

For a given temporal frequency, input-output analysis generates the optimal and and several sub-optimal modes sorted by their corresponding gains. Figure 2 shows the first 50 singular values for the $M_j = 1.5$ jet with $T_j/T_\infty = 1.44$, or equivalently $M_a = 1.8$, for the forcing frequency $St = 0.28$. The optimal gain for this heated jet is found to be $\sigma_1 = 3.26 \times 10^2$, which is larger than that for the isothermal jet with the same jet Mach number.

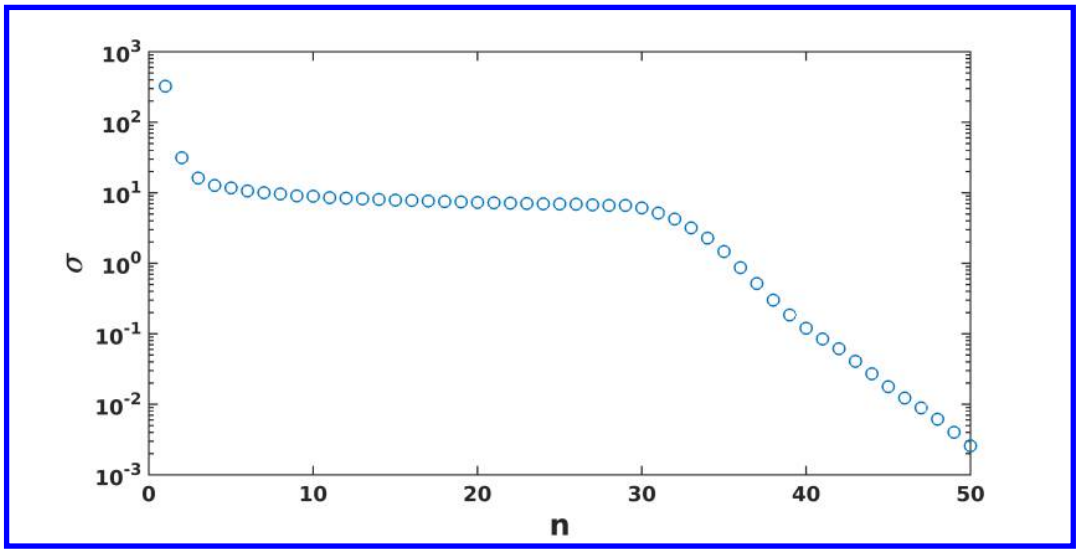

Figure 2. Singular values vs. mode number for the $M_j = 1.5$ jet with $T_j/T_\infty = 1.44$ at forcing frequency $St = 0.28$.

Figure 3 and figure 4 respectively visualize the first four output and input modes for the heated jet. The output modes, which are restricted to be pressure perturbations in the region far away from the jet, follow the same pattern as shown in the case of isothermal jet in terms of the number of beams and corresponding radiation angles with respect to the mode number. The optimal mode shows a single strong acoustic beam radiating at an angle of 32° in the direction of peak jet noise measured from the downstream jet axis, which is slightly larger than the isothermal case. As the mode number increases, additional beams appear at both larger and smaller radiation angles.

The input modes are restricted to the region near to the jet turbulence, as represented by the rectangle in figure 4. The choice of the input domain is also consistent with the study of input-output analysis for isothermal jets. Compared to that obtained for the isothermal jet, the optimal input mode in this case is more highly concentrated upstream of the nozzle exit. Similar to the isothermal sub-optimal input modes, sub-optimal inputs for this heated jet extend downstream farther than the optimal mode. It is found that the sub-optimal inputs for the heated jet, however, align better with the shear layer in comparison with those obtained for the isothermal case.

We repeat input-output analysis for a $M_j = 0.9$ subsonic heated jet with $T_j/T_\infty = 1.78$, or equivalently $M_a = 1.2$, for the forcing frequency $St = 0.42$. This jet Strouhal number yields the same acoustic Strouhal number $St_a = StM_a = 0.50$ as the case of the heated supersonic jet examined earlier. This is important because the acoustic Strouhal number was found to be a new dimensionless variable to predict the input-output behavior of jet noise.[11]

Figure 5 visualizes the first two output modes for the subsonic heated jets. While output modes show the same pattern as the supersonic heated jet, the direction of peak jet noise in this case is aligned at smaller angle of 20° as shown in figure 5(a).

In the study of input-output analysis for isothermal jets, authors showed that the optimal and the first sub-optimal ($n = 2$) input modes extended farther downstream of the nozzle exit. Unlike the subsonic isothermal jet case, figure 6(a) shows that the optimal inputs of this heated jet are extremely confined to the vicinity of the nozzle exit. While the first sub-optimal mode shown in figure 6(b) extends farther downstream,

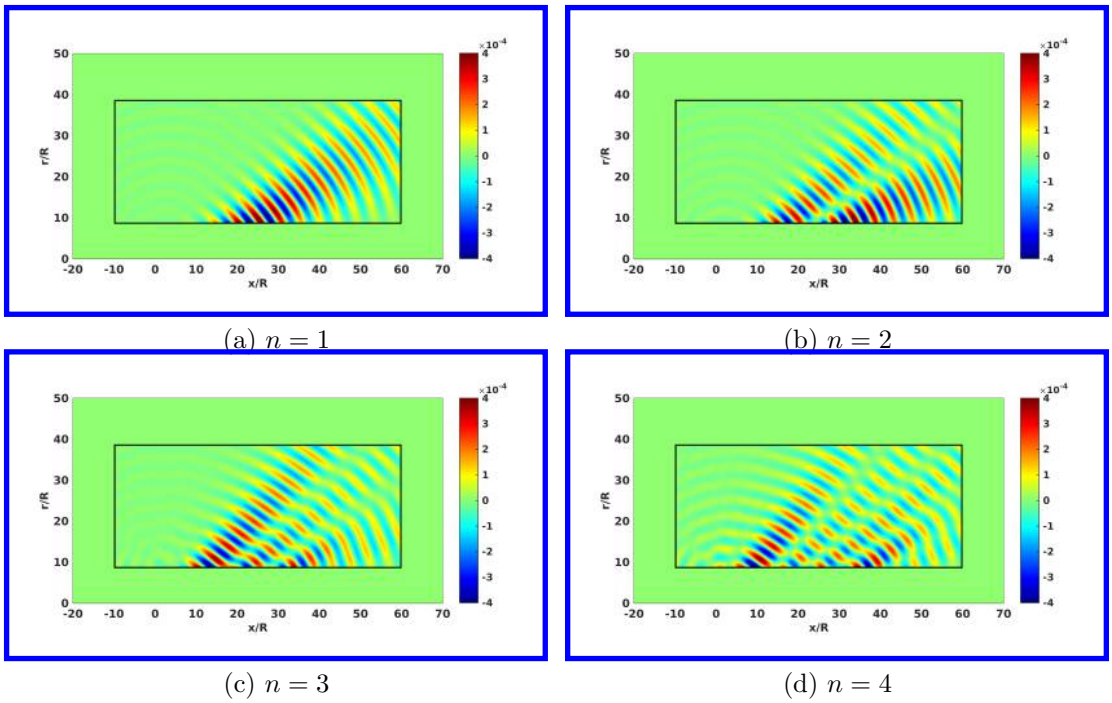

(a) $n = 1$ (b) $n = 2$

(c) $n = 3$ (d) $n = 4$

Figure 3. The first four input modes of the $M_j = 1.5$ supersonic heated jet with $T_j/T_\infty = 1.44$. Contours visualize the real part of the normalized output pressure perturbations for forcing frequency $St = 0.28$.

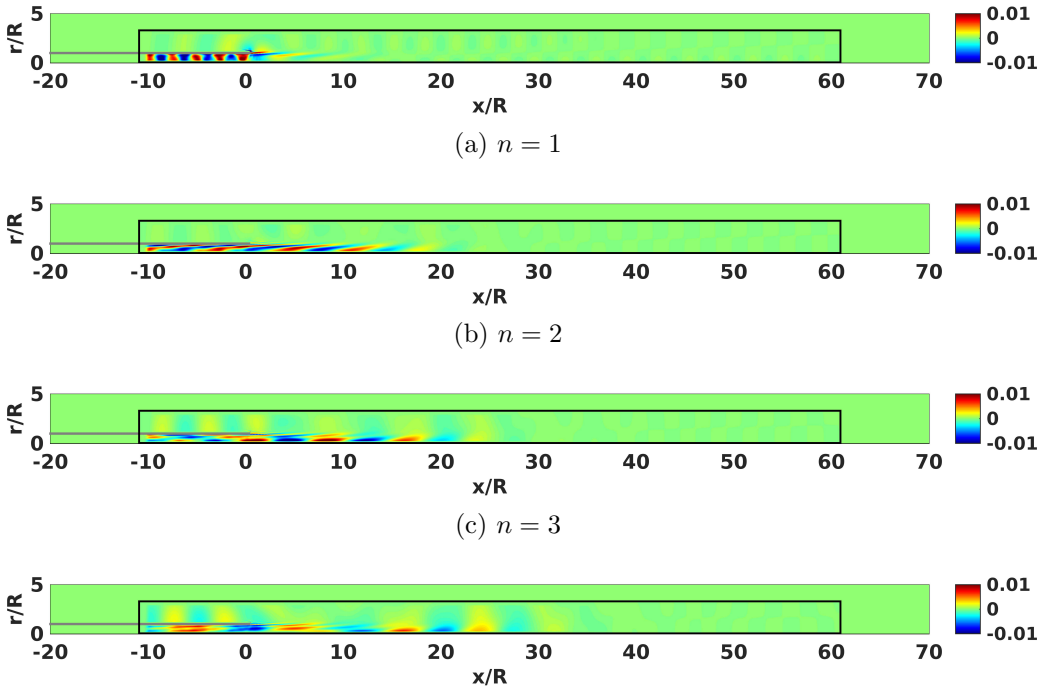

(a) $n = 1$

(b) $n = 2$

(c) $n = 3$

(d) $n = 4$

Figure 4. The first four input modes of the $M_j = 1.5$ supersonic heated jet with $T_j/T_\infty = 1.44$. Contours visualize the real part of the normalized axial velocity forcings for forcing frequency $St = 0.28$. normalized

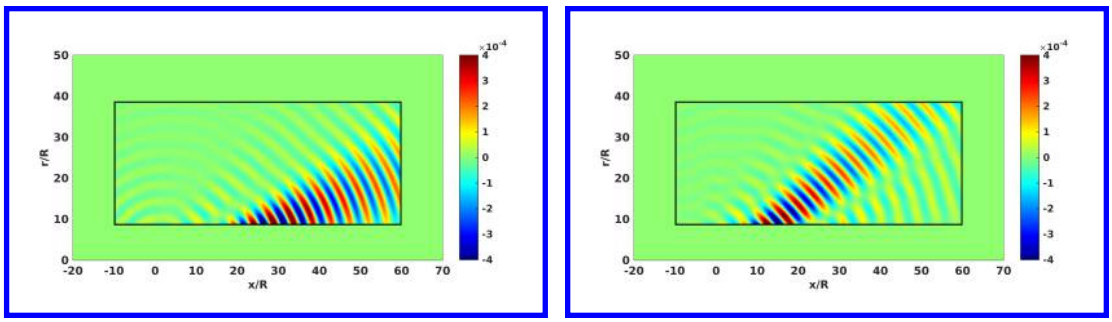

(a) $n = 1$ (b) $n = 2$

Figure 5. The first two input modes of the $M_j = 0.9$ subsonic heated jet with $T_j/T_\infty = 1.78$. Contours visualize the real part of the normalized output pressure perturbations for forcing frequency $St = 0.42$.

it is still shifted upstream, compared to the isothermal subsonic jet with the same jet Mach number. This indicates that applied heating makes a subsonic jet behave more like a supersonic jet; in other words, in the heated subsonic jet the largest singular value may be much greater than the second singular value. Figure 7 shows singular values vs. mode number for this subsonic heated jet and confirms that optimal gain increases with applied heating. Note that the first few sub-optimal gains were comparable to the optimal gain in isothermal subsonic jets.

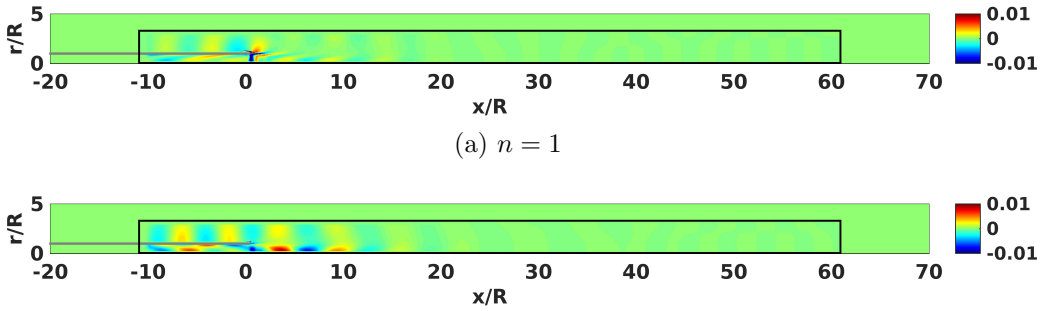

(a) $n = 1$

(b) $n = 2$

Figure 6. The first four input modes of the $M_j = 0.9$ supersonic heated jet with $T_j/T_\infty = 1.78$. Contours visualize the real part of the normalized axial velocity forcings for forcing frequency $St = 0.42$. normalized

B. Sound pressure level increase with applied heating

In a previous study, it was shown that including sub-optimal modes recovers a fraction of the missing sound.[11] To investigate the effect of heating on the sound recovery by sub-optimal modes, we consider 28 RANS base flows whose jet Mach number and acoustic Mach number vary such that $0.6 < M_j < 1.5$ and $0.6 < M_a < 1.8$. The amount of recovery may be quantified in decibel scale as the sound pressure level increase ΔSPL obtained by including sub-optimal modes vs. retaining the only optimal mode:

$$\Delta SPL = 10 \log_{10} \left(\frac{\sum \sigma_n^2}{\sigma_1^2} \right). \tag{12}$$

Figure 8 shows SPL increase with respect to different acoustic Mach number for a fixed jet Mach number. Heated jets represented by open markers follow remarkably well the SPL increase fashion of the isothermal case (black closed squares), and this thus implies that applied heating triggers the onset of Mach wave radiation. This result also agrees with the change of patterns of input and output modes we observed for the subsonic heated jet with $M_j = 0.9$ and $T_j/T_\infty = 1.78$.

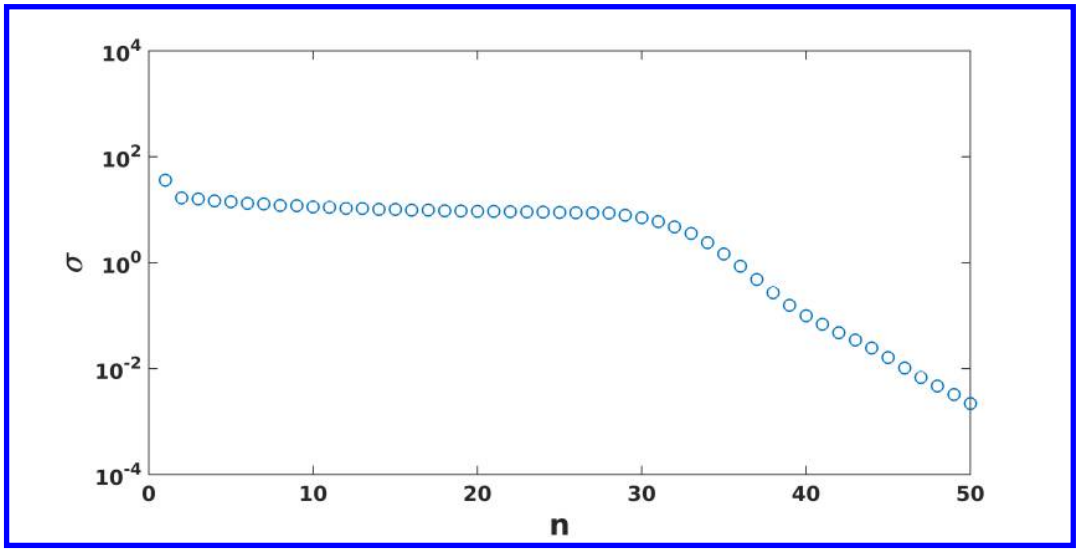

Figure 7. Singular values vs. mode number for the $M_j = 0.9$ jet with $T_j/T_\infty = 1.78$ at forcing frequency $St = 0.42$.

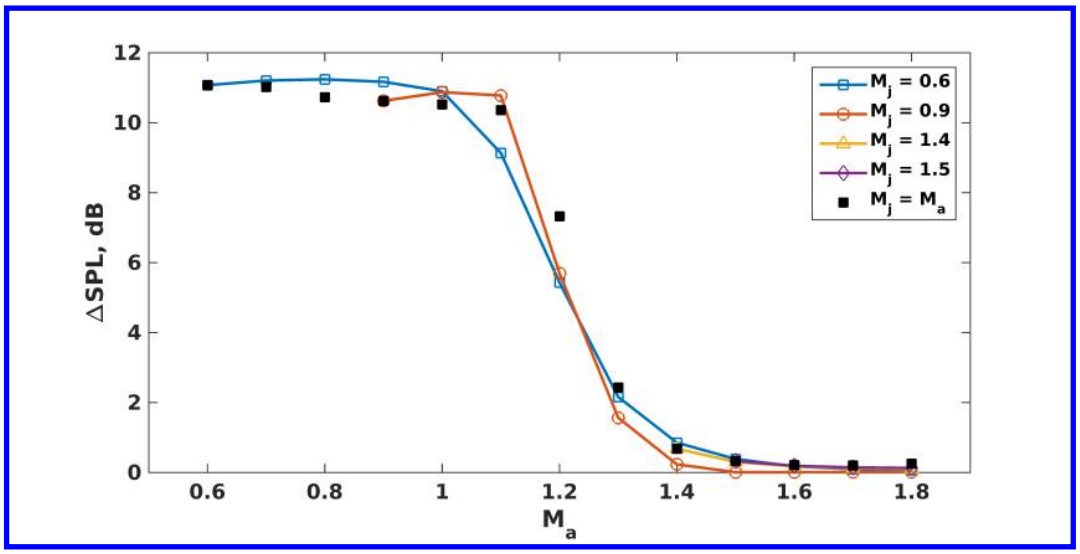

Figure 8. SPL increase vs. acoustic Mach number for a fixed acoustic Strouhal number $St_a = 0.50$. Black closed squares represent the result of isothermal jets and open markers show results corresponding to each jet Mach number.

C. Role of the acoustic Strouhal number

The singular values computed using input-output analysis follow a particular pattern; after the first few modes sub-optimal gains reach a plateau that is maintained across many mode numbers. Gains then suddenly start decreasing again. A previous study found that the acoustic Strouhal number St_a controls the number of sub-optimal modes with significant gains.[11] By examining heated jets with various jet Mach numbers and jet-to-ambient temperature ratios, we see that the acoustic Strouhal number can predict the sudden drop of gains, regardless of the amount of applied heating as shown in figure 9.

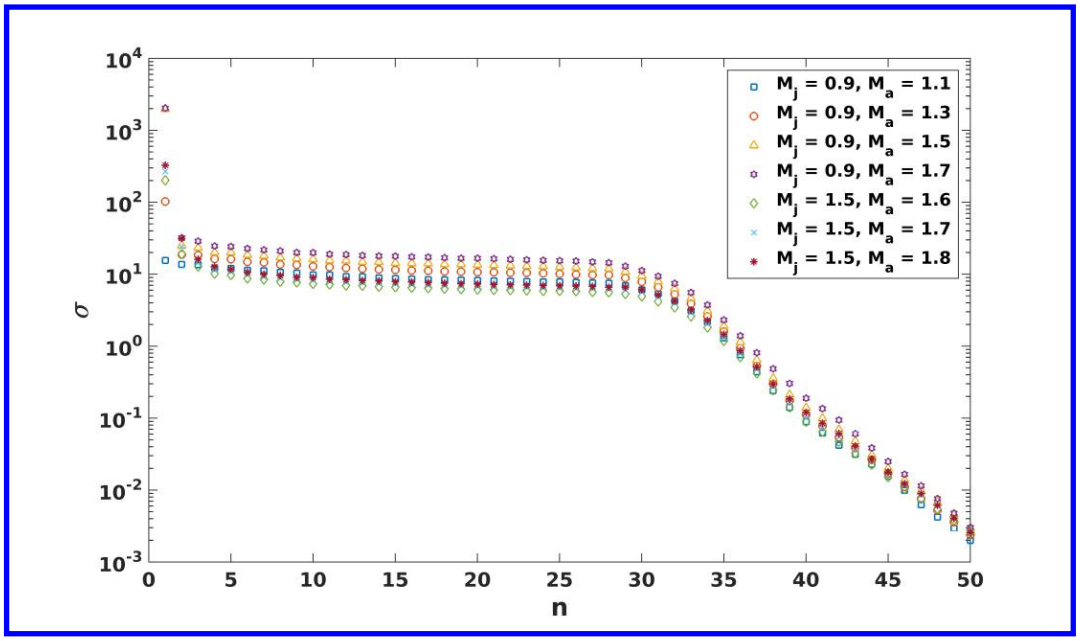

Figure 9. Singular values vs. mode number for heated jets with different jet-to-ambient temperature ratios keeping the acoustic Strouhal number fixed $St_a = 0.50$. Among 28 different heated jets tested, results of few selected base flows are shown.

While the acoustic Strouhal number retain the ability to predict the sudden drop of gains for heated jets as in the case of isothermal jets, in figure 9 sub-optimal singular values for different base flows do not collapse to a single curve. As the amount of applied heating increases, the optimal and sub-optimal singular values shift upward. In contrast to sub-optimal singular values which strictly increase with more heating, the corresponding optimal gains start to converge as the jet-to-ambient ratio goes beyond a certain value. For some cases, this may result in the rise in ΔSPL including sub-optimal modes over some jet-to-ambient ratio (ΔSPL increases again after $M_a > 1.6$ for the $M_j = 0.9$ jet).

D. Effects of heating on sub-optimal modes

One motivation for the present study was the fact that PSE analysis underpredicts the far-field acoustics, especially in the sideline direction.[5] We considered many RANS solutions of turbulent jets with different jet Mach numbers and amounts of applied heating as base flows to examine whether input-output analysis is able to recover the missing sound in such cases. The results shown in previous sections, however, seem to support that applied heating is in fact beneficial to PSE analysis. This contradiction may result from the assumption that the jet turbulence excites all modes with equal amounts of forcing. To quantify the relevance of sub-optimal modes of heated jets in the presence of realistic forcing, we therefore project high-fidelity LES data onto input modes.

The LES database we utilize was obtained for $M_j = 1.5$ supersonic jet heated with $T_j/T_\infty = 1.74$ and 5.1% axial co-flow using an unstructured finite-volume compressible flow solver. Further details may be found in Ref. 23. We take the time average of $5,000$ snapshots taken from the LES with time intervals of $0.02D/c_\infty$. We also take an average of the database in the azimuthal direction. The numerical domain of the LES extends from $x/R = 0$ to 40 and $r/R = 0$ to 10, in the axial and radial directions, respectively. As explained earlier, the RANS solutions was obtained for a larger numerical domain than the LES domain. To

account for the difference in numerical domains between two base flows, the LES base flow was extrapolated to the RANS domain, and the input and output domains were restricted to $x/R = 40$ in the axial direction.

Despite differences between the two base flows, figure 10 shows that the resulting singular values of two base flows agree very well. The largest differences occur for the optimal gain as well as for the sub-optimal gains near the dropoff location. Whereas the optimal singular value of the LES base flow is observed to be 1.51 times greater than that of the RANS base flow, sub-optimal singular values of the LES base flow after $n \approx 20$ are slightly smaller than those obtained from the RANS base flow. Considering the definition of SPL increase by including sub-optimal modes given by equation (12), this implies that the contribution of sub-optimal modes in this case becomes less significant. We therefore think of the results of the LES base flow as lower bounds for this jet.

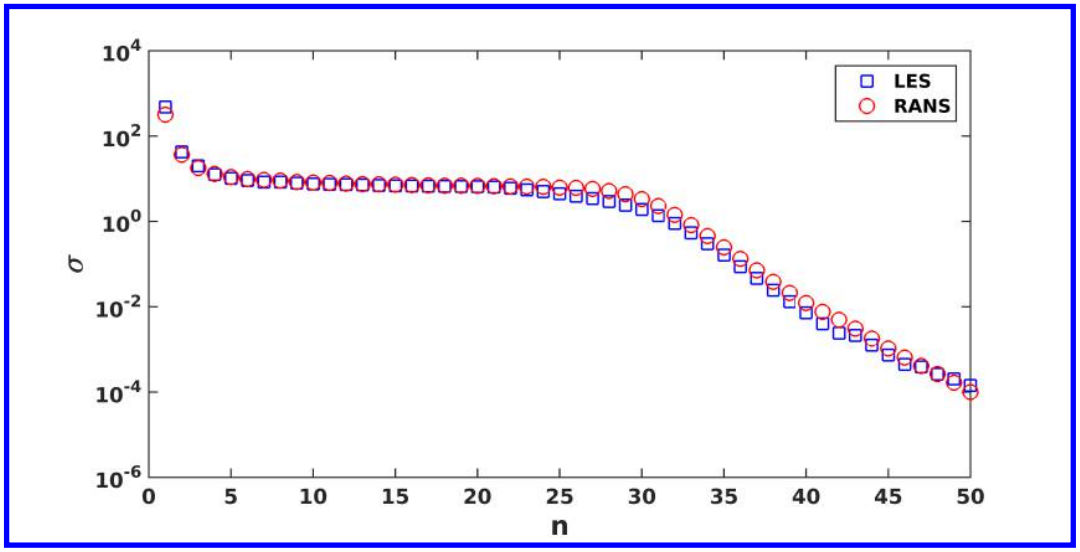

Figure 10. Singular vslues vs. mode number for the $M_j = 1.5$ jet with $T_j/T_\infty = 1.74$ for forcing frequency $St = 0.33$.

By decomposing the velocity and the density in equations (2) into mean and fluctuating parts, subtracting base flow terms, and further taking Fourier transforms, the nonlinear source term $\hat{q}_{LES}$ may be written as:

$$\hat{q}_{LES} = FFT\left(\frac{\rho'\nabla p'}{\bar{\rho}(\bar{\rho}+\rho')} - \boldsymbol{u'}\cdot\nabla\boldsymbol{u'}\right). \tag{13}$$

This term can be viewed as the input forcing f deriving the linearized velocity equations (4). By projecting the forcing onto the orthonormal set of input modes $q_{in,n}$, the relevance of input modes in the presence of realistic forcing is quantified in the form of amplitudes as:

$$a_n = \langle \hat{q}_{LES}, q_{in,n} \rangle . \tag{14}$$

For the $M_j = 1.5$ jet with $T_j/T_\infty = 1.74$ for forcing frequency $St = 0.33$, the amplitudes normalized by the average amplitude of the LES source are shown in figure 11. Note that the amplitudes of sub-optimal modes are much larger than the amplitude of the optimal mode, and thus sub-optimal input modes are physically relevant to the realistic forcing.

Finally, we modulate the singular values obtained with the assumption of white noise forcing σ_n by the input amplitudes a_n computed from the LES projection. This process produces effective gains given as:

$$\sigma_{eff,n} = \sigma_n a_n, \tag{15}$$

which quantify the contribution of sub-optimal modes with realistic forcing as shown in figure 12. Without the LES forcing, SPL increase by including sub-optimal modes was computed as 0.14 dB. In the presence of realistic forcing, however, ΔSPL jumps to 7.92 dB which represents a remarkable increase when considering the logarithmic decibel scale.

At the beginning of this section, we pointed out that the results obtained from the white noise forcing may imply that applied heating is advantageous to PSE analysis; this contradicts the underprediction of

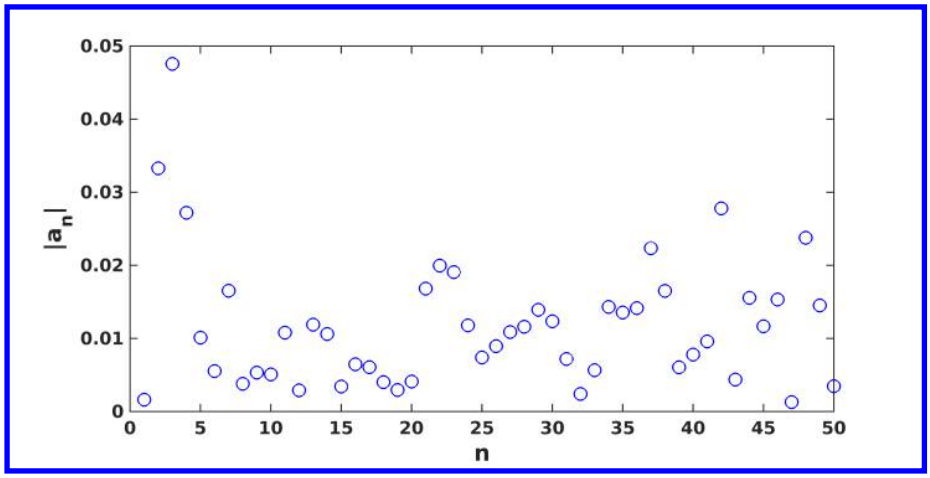

Figure 11. Amplitudes $|a_n|$ are determined by projecting the LES forcing onto the orthonormal set of input modes for the $M_j = 1.5$ jet with $T_j/T_\infty = 1.74$ and the azimuthal wavenumber $m = 0$ for forcing frequency $St = 0.33$.

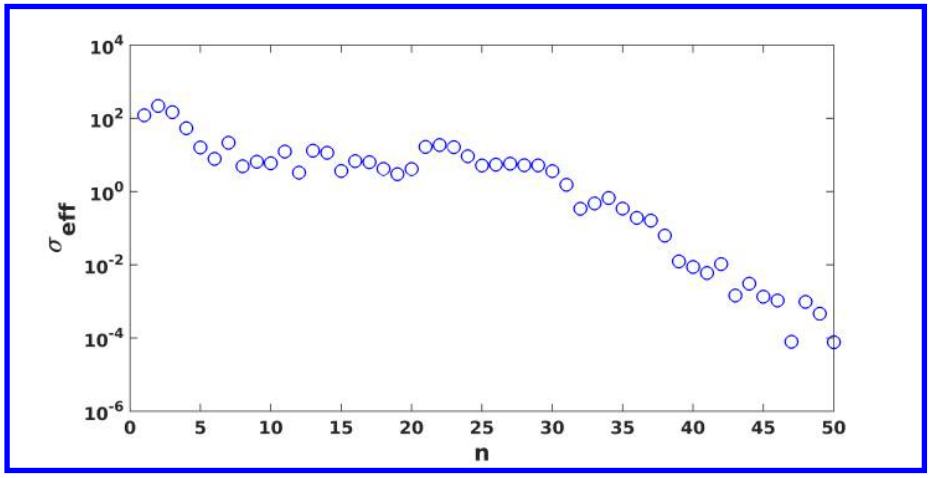

Figure 12. Effective gains determined by projecting the LES forcing onto the orthonormal set of input modes for the $M_j = 1.5$ jet with $T_j/T_\infty = 1.74$ and the azimuthal wavenumber $m = 0$ for forcing frequency $St = 0.33$. Singular values obtained with the white noise forcing are modulated by the input amplitudes a_n computed from the LES projection.

PSE analysis for supersonic heated jets. Using the LES projection, we demonstrate that sub-optimal modes are very significant with realistic forcing for the $M_j = 1.5$ jet with applied heating, and this may explain why PSE analysis cannot successfully capture the far-field sound of supersonic heated jets.

IV. Conclusion

In this paper, we consider input-output analysis of small perturbations about RANS and LES base flows for axisymmetric, heated, high-speed, turbulent jets. For a given temporal forcing frequency, input-output analysis yields the optimal and sub-optimal modes associated with the largest singular value and lesser singular values, respectively, and they preserve coherent structures similar to what we observe for isothermal jets. By including the contribution of sub-optimal modes, input-output analysis enables the noise prediction of heated jets.

By examining various RANS solutions with jet and acoustic Mach numbers ranging $0.6 < M_j < 1.8$ and $0.6 < M_a < 2.0$, we find that applied heating triggers disturbances to propagate through Mach wave radiation because the convection velocity of instability waves with respect to the ambient speed of sound lies in the supersonic regime in such cases. As the amount of applied heating increases, the optimal gain becomes much larger than sub-optimal gains. In this sense, one may think that applied heating in fact benefits PSE analysis. It should be noted that, however, this argument results from the assumption of white noise forcing. By projecting the LES database onto a basis of input modes, we observe that sub-optimal modes are even more relevant in the presence of realistic forcing. For the $M_j = 1.5$ heated jet with $T_j/T_\infty = 1.74$ for forcing frequency $St = 0.33$, ΔSPL owing to sub-optimal modes is found to be 7.92 dB. This is indeed a huge increase, compared to 0.14 dB which is obtained assuming all singular directions being forced equally. We also find that acoustic Strouhal number still controls the dropoff location of sub-optimal singular values after the plateau as in the case of isothermal jets.

Acknowledgments

This research was supported in part by the Aerospace Engineering and Mechanics Departments faculty startup fund at the University of Minnesota, the University of Minnesota Informatics Institute Transdisciplinary Faculty Fellowship, and the National Science Foundation under Award No. CMMI 1363266. High-fidelity simulations were enabled by grants of computer time at the ERDC and AFRL supercomputing centers as well as at the Argonne National Laboratory.

References

[1]Mollo-Christensen, E., "Measurements of near field pressure of subsonic jets," Tech. rep., Advisory Group for Aeronautical Research and Development, 1963.

[2]Cheung, L. C., Bodony, D. J., and Lele, S. K., "Noise radiation predictions from jet instability waves using a hybrid nonlinear PSE-acoustic analogy approach," *AIAA Paper 2007-3638*, 2007.

[3]Gudmundsson, K. and Colonius, T., "Instability wave models for the near-field fluctuations of turbulent jets," *Journal of Fluid Mechanics*, Vol. 689, 2011, pp. 97–128.

[4]Rodríguez, D., Sinha, A., Brès, G. A., and Colonius, T., "Inlet conditions for wave packet models in turbulent jets based on eigenmode decomposition of large eddy simulation data," *Physics of Fluids*, Vol. 25, No. 10, 2013, pp. 105–107.

[5]Sinha, A., Rodríguez, D., Brès, G. A., and Colonius, T., "Wavepacket models for supersonic jet noise," *Journal of Fluid Mechanics*, Vol. 742, 2014, pp. 71–95.

[6]Jordan, P. and Colonius, T., "Wave packets and turbulent jet noise," *Annual Review of Fluid Mechanics*, Vol. 45, 2013, pp. 173–195.

[7]Nichols, J. W. and Lele, S. K., "Global modes and transient response of a cold supersonic jet," *Journal of Fluid Mechanics*, Vol. 669, 2011, pp. 225–241.

[8]Schmid, P. J. and Henningson, D. S., *Stability and transition in shear flows*, Vol. 142 of *Applied mathematical sciences*, Springer, 2001.

[9]Garnaud, X., Lesshafft, L., Schmid, P., and Huerre, P., "The preferred mode of incompressible jets: linear frequency response analysis," *Journal of Fluid Mechanics*, Vol. 716, 2013, pp. 189–202.

[10]Nichols, J. W. and Jovanović, M. R., "Input-output analysis of high-speed jet noise," *Proceedings of the Summer Program*, Center for Turbulence Reearch, Stanford University, 2014, pp. 251–260.

[11]Jeun, J., Nichols, J. W., and Jovanović, M. R., "Input-output analysis of high-speed axisymmetric isothermal jet noise," *Physics of Fluids*, Vol. 28, No. 4, 2016.

[12]Papamoschou, D., "Wavepacket modeling of the jet noise source," *AIAA Paper 2011-2835*, 2011.

[13]Jovanović, M. R. and Bamieh, B., "Componentwise energy amplification in channel flows," *Journal of Fluid Mechanics*, Vol. 534, 2005, pp. 145–183.

[14]Thies, A. T. and Tam, C. K., "Computation of turbulent axisymmetric and nonaxisymmetric jet flows using the k-ε model," *AIAA journal*, Vol. 34, No. 2, 1996, pp. 309–316.

[15]Crighton, D. and Gaster, M., "Stability of slowly diverging jet flow," *Journal of Fluid Mechanics*, Vol. 77, No. 02, 1976, pp. 397–413.

[16]Jameson, A., "Aerodynamic design via control theory," *Journal of scientific computing*, Vol. 3, No. 3, 1988, pp. 233–260.

[17]Jameson, A., "Re-engineering the design process through computation," *Journal of Aircraft*, Vol. 36, No. 1, 1999, pp. 36–50.

[18]Newman III, J. C., Taylor III, A. C., Barnwell, R. W., Newman, P. A., and Hou, G. J.-W., "Overview of sensitivity analysis and shape optimization for complex aerodynamic configurations," *Journal of Aircraft*, Vol. 36, No. 1, 1999, pp. 87–96.

[19]Chandler, G. J., Juniper, M. P., Nichols, J. W., and Schmid, P. J., "Adjoint algorithms for the Navier-Stokes equations in the low Mach number limit," *Journal of Computational Physics*, Vol. 231, No. 4, 2012, pp. 1900–1916.

[20]Khalighi, Y., Mani, A., Ham, F., and Moin, P., "Prediction of sound generated by complex flows at low Mach numbers," *AIAA journal*, Vol. 48, No. 2, 2010, pp. 306–316.

[21]Mani, A., "Analysis and optimization of numerical sponge layers as a nonreflective boundary treatment," *Journal of Computational Physics*, Vol. 231, No. 2, 2012, pp. 704–716.

[22]Lehoucq, R. B., Sorensen, D. C., and Yang, C., *Users' Guide: Solution of Large-Scale Eigenvalue Problems with Implicitly Restarted Arnoldi Methods*, SIAM, 1998.

[23]Brès, G. A., Nichols, J. W., Lele, S. K., and Ham, F. E., "Towards best practices for jet noise predictions with unstructured large eddy simulations," *AIAA Paper 2012-2965*, 2012.